Neuropsychiatric Disease and Treatment

Dovepress

open access to scientific and medical research

Open Access Full Text Article

STUDY PROTOCOL

Proteomic Analysis Reveals that Di Dang Decoction Protects Against Acute Intracerebral Hemorrhage Stroke in Rats by Regulating S100a8, S100a9 Col1a1, and Col1a2

Lina Feng[1]
Mingquan Li[2]
Jixiang Ren[3]
Yujuan Li[4]
Qi Wang[5]
Pengqi Zhang[1]
Xinyue Zhang[1]
Tianye Wang[5]
Yunqiang Li[1]

[1]College of Traditional Chinese Medicine, Changchun University of Chinese Medicine, Changchun, Jilin Province, People's Republic of China; [2]Neurology Department, Third Affiliated Clinical Hospital of Changchun University of Traditional Chinese Medicine, Changchun, Jilin Province, People's Republic of China; [3]Preclinical Department, Affiliated Hospital of Changchun University of Traditional Chinese Medicine, Changchun, Jilin Province, People's Republic of China; [4]Ultrasonic Diagnosis Department, Third Affiliated Clinical Hospital of Changchun University of Traditional Chinese Medicine, Changchun, Jilin Province, People's Republic of China; [5]College of Integrated Chinese and Western Medicine, Changchun University of Chinese Medicine, Changchun, Jilin Province, People's Republic of China

Objective: The present study aimed to explore the neuroprotective mechanism of Di Dang decoction (DDD) during acute intracerebral hemorrhage (AICH) stroke in Sprague Dawley rats through proteomic analysis.

Methods: A total of 135 healthy Sprague Dawley rats were randomly divided into five groups: control (n = 27), model (n = 27), DDD low-dose (n = 27), DDD medium-dose (n = 27), and DDD high-dose (n = 27). AICH stroke in rats was induced by injecting autologous blood into the caudate nucleus. The modified Neurological Severity Score (mNSS) was used to evaluate the cerebral nerve function deficit. Hematoxylin and eosin (HE) staining was performed to observe the brain tissue at the lesion site. Albumin concentration was assessed on obvious blood-brain barrier damaged and brain water content was used to evaluate the brain injury. For quantitative proteomics, proteins were extracted from the cerebral cortices. Target proteins were identified using mass spectrometer-based targeted proteomic quantification.

Results: mNSS score, HE staining results, albumin concentration, and brain water content showed the most significant improvements in the neuroprotective in the high-dose group 7 days after DDD exposure. Furthermore, quantitative proteomics analysis showed that, relative to the control group, S100a8 and S100a9 were downregulated by 0.614 (p = 0.033702) and 0.506 times (p = 0.000024) in the high-dose group. Compared with the control group, Col1a1 and Col1a2 were upregulated by 1.319 (p = 0.000184) and 1.348 (p = 0.014097) times in the high-dose group. These results were confirmed using mass spectrometer-based targeted proteomic quantification.

Conclusion: Application of a high-dose DDD for 7 days in AICH stroke rats showed the most significant improvements in neuroprotective. Mechanistically, this effect was mediated by S100a8 and S100a9 protein downregulation and Col1a1 and Col1a2 upregulation.

Keywords: acute intracerebral hemorrhage stroke, S100a8, S100a9, Col1a1, Col1a2, Di Dang decoction

Introduction

Background

Stroke, a cerebrovascular accident, is a clinical event associated with focal or diffuse brain function deficits caused by acute cerebral circulation disturbance. Stroke is also the second leading cause of death in urban and rural residents

Correspondence: Mingquan Li
Tel +86-15543120222
Email liminhquan0001@126.com

Received: 29 July 2021
Accepted: 30 October 2021
Published: 10 November 2021

diagnosed with malignant tumors.[1] There are two main categories of stroke according to their pathological properties: ischemic stroke and hemorrhagic stroke. Intracerebral hemorrhage (ICH) refers to a hemorrhage in the brain parenchyma and is characterized by rapid onset, neurological deterioration, and poor outcome.[2] Acute intracerebral hemorrhage (AICH) was observed in 23.4% of patients who had a stroke in China, 46% of whom have died or suffered a severe disability within one year,[3] and 36% of survivors remained moderately to severely disabled at discharge.[4] Many modifiable risk factors, including arterial hypertension, excessive consumption, decreased low-density lipoprotein cholesterol, and low serum triglyceride levels, can cause AICH.[5] Conventional therapies for AICH include hematoma removal, edema attenuation, and intracranial pressure reduction. However, contrary to expectations, the effectiveness of therapy is unsatisfactory.[6] Therefore, it is necessary to develop new strategies to treat ICH.

Purpose

Traditional Chinese Medicine (TCM) has been shown positively effect on stroke.[6] Professor Ren Jixue, who has made remarkable contributions in TCM encephalopathy, especially in emergency cases, established the remarkably effective method of "removing blood stasis" to treat hemorrhagic stroke. In particular, Di Dang decoction (DDD) is a classical TCM prescription for acute hemorrhagic stroke and is representative prescription to "remove blood stasis," which comes from the "Treatise on febrile diseases". Specifically, DDD promotes blood circulation and removes blood stasis, effectively purging and clearing the viscera. DDD includes rhubarb (Latin name: *Rheum palmatum L*), peach kernel (Latin name: *Prunus persica L. Batsch*), leech (Latin name: *Whitmania pigra Whitman*), and gadfly (Latin name: *Tabanus mandarinus Schiner*). Using DDD to treat AICH has a long history of demonstrated effective clinical therapeutic effects. Our previous study showed that DDD significantly reduced brain water content and intracerebral hematoma volume in rats with ICH by up-regulating the expression of brain-derived neurotrophic factor, tyrosine kinase B and vascular endothelial growth factor (VEGF).[7] Previous study also showed that Di Dang decoction inhibits endoplasmic reticulum stress-mediated apoptosis induced by oxygen glucose deprivation and intracerebral hemorrhage through blockade of the GRP78-IRE1/PERK pathways.[8] We also found that the protective effect of Di Dang decoction against AlCl 3-induced oxidative stress and apoptosis in PC12 cells through the activation of SIRT1-Mediated Akt/Nrf2/HO-1pathway.[9] In addition, previous reports showed that leech alcohol extract and rhubarb water extract alleviated the inflammation of peripheral tissue and cerebral edema in rats with ICH.[10,11] Peach seed water extract up-regulated VEGF and VEGF receptor 2 after ICH in a mouse model[6] and inhibited glucose deprivation injury in PC12 cells.[12] However, its specific molecular mechanism of protecting against acute intracerebral hemorrhage stroke in rats remains unclear. This study aimed to investigate the effect of DDD on AICH stroke rats and to clarify its mechanism of action to guide its clinical use.

Methods

Animal Maintenance

The experimental animal protocol was approved by the Animal Ethics Committee of Changchun University of Traditional Chinese Medicine (Approval No.: 20180008). All animal experimental procedures were performed in accordance with the guidelines of the National Institutes of Health on the care and use of animals. Animals were housed in an Association for Assessment and Accreditation of Laboratory Animal Care International (AAALAC)-approved animal quarters in our hospital. Studies were carried out on adult Sprague Dawley (SD) rats (180–220 g, 8–10 weeks of age) obtained from Changchun Yi si Laboratory Animal Technology Co. Ltd. All animals were housed under identical conditions (room temperature at 25 °C and 12/12 h light/dark cycle), and allowed ad libitum access to food and water. Before inducing the AICH model, all rats were fed for one week.

DDD Preparation and HPLC Fingerprint Analysis

According to the original prescription from the "TCM prescriptions dictionary," DDD is composed of four Chinese components: rhubarb (Chinese name: Dahuang, Latin name: *Rheum palmatum L*, Family: Polygonaceae, Batch number: 170916, Part used: root and rhizome), peach kernel (Chinese name: Taoren, Latin name: *Prunus persica L. Batsch*, Family: Rosaceae, Batch number: 171011, Part used: seed), leech (Chinese name: Shuizhi, Latin name: *Whitmania pigra Whitman*, Family: Hirudinidae, Batch number: 170824, Part used: whole animal), and gadfly (Chinese name: Mengchong, Latin name: *Tabanus mandarinus Schiner*, Family: Tabanidae,

Batch number: 171015, Part used: whole animal). All dried components were purchased from the Affiliated Hospital of the Changchun University of Chinese Medicine and identified through the department of Medicine. First, the herbs were minced, mixed, soaked for 30 min in distilled water, and then decocted in distilled water at 100 °C for 30 min. The above procedure was repeated three times, merging decoctions, and increasing the concentration. The concentrated solution was freeze-dried under a vacuum and grounded into a powder. According to the ratio of equivalent dose converted by body surface area between human and rat, the powder was dissolved in distilled water to final concentrations of 0.625 g/mL (high-dose), 0.3125 g/mL (medium-dose), and 0.15625 g/mL (low-dose) for later use.

As our team reported,[8,9] we have established a method for the detection of active ingredients from DDD via high-performance liquid chromatography (HPLC, Agilent, Santa Clara, CA, US). Eighteen major peaks of DDD extract were identified using HPLC. Gallic acid, amygdalin, sennoside B, rhein-8-glucoside, sennoside A, emodin, chrysophanol, aloe-emodin, and rhein in DDD were identified by comparing the retention time from high-performance liquid chromatography with good reproducibility.

Experimental Animal Grouping

A total of 135 healthy SD rats were randomly assigned to five groups: control, model, DDD low-dose, DDD medium-dose, and DDD high-dose groups. Twenty-seven healthy SD rats were used in each group. Each group was further divided into three subgroups, each of which contained at least nine rats.

AICH Stroke Model Establishment

The model, low-, medium-, and high-dose groups were intraperitoneally injected using a posterior pituitary injection of 2 U/kg once daily for 14 days. After 14 days, the modified Nath method was used to replicate the AICH model.[8] Rats were intraperitoneally injected with 1% sodium pentobarbital, fixed in the supine position. The skin was prepared, the femoral artery was separated, and its distal end was ligated. Furthermore, 50 μL of femoral arterial blood was extracted, the artery was then ligated and surgically sutured. Subsequently, rats were fixed in a stereoscopic brain locator; the skin was prepared and routinely disinfected, the anterior fontanelle was separated, the caudate nuclear was localized, and 50 μL of autologous blood were slowly injected. After the operation, the scalp was sutured and coated with penicillin powder. The control group underwent the same procedure excluding the injection of autologous blood into the caudate nucleus.

Determination of model success: after the rats were fully alert following surgery, the modified Neurological Severity Score (mNSS)[13] was used to evaluate the neurological deficit of ICH model rats; an mNSS score > 6, and hematoma formation could be seen in the perfused brain tissue, indicating that the model was successfully established. If the symptoms of neurological impairment were too mild, absent, or too great, rats with impaired consciousness, difficulty in moving, or that died, they were discarded. Gavage was given immediately after successful modeling according to their respective dose concentrations; while DDD in the control and model groups was replaced with an equivalent dose of normal saline (each group was administered 1 mL/100 g of body weight gavage intragastrically once a day at the same time).

Rats in each group were sacrificed at 1, 3, and 7 days after drug administration; then, the cerebral cortex of the affected side was isolated.

Evaluating DDD on the Neurological Outcomes in AICH Rats

Two observers, blinded to the experimental design, scored the animals independently, and scores were averaged. The tests were composed of a modified Neurological Severity Score (mNSS)[13] and repeated three times. mNSS neurological score: an eighteen-point neurological score was employed (normal score 0; maximal deficit score 18). For the injury severity score, one point was scored for the inability to perform the test or the lack of a tested reflex. Thus, the higher the score, the more severe the injury.

Hematoxylin and Eosin (HE) Staining Method

(a) After paraffin-embedded sections were heated, a xylene gradient was used to dewax samples, and gradient ethanol solutions were added to remove xylene.
(b) Sections were placed in hematoxylin for 5–7 min, then washed with water for 1 min.
(c) Hydrochloric acid alcohol (1%) was added for 10–30 s (depending on tablets), then washed under running water for 5–10 s.

(d) The sections were placed in a saturated aqueous solution of lithium carbonate back blue for 10–30 s, soaked under tap water for 5–10 min, and soaked in eosin solution for 20 min. Finally, sections were washed for 1 min.
(e) Samples were then dehydrated using gradient alcohol solutions, placed in fresh xylene, cleared to achieve transparency, and sealed using neutral gum.
(f) Pathological changes were observed under a light microscope.

BBB (Blood-Brain Barrier) Injury and Brain Water Content

BBB permeability was assessed on the basis of album extravasation.[14] Generally, albumin concentration in the brain is very low because of the existence of BBB, but the content of albumin in the brain tissues increases obviously once BBB damaged. Therefore, the changes of albumin conversion can serve as an indicator to estimate the degree of BBB injury.[15,16] Western blot analysis was used to test the protein levels of albumin in brain tissues of rats in each group.

Western blot analysis: Briefly, brain samples around the hematoma were collected, homogenized, and lysed separately in ice-cold RIPA lysis buffer (Beyotime, China). Then the samples were centrifuged for 10 min (4 °C, 12,000 g). The supernatants were collected immediately and the protein concentrations were determined using a bicinchoninic acid (BCA) kit (Beyotime, China) according to the manufacturer's instructions. The protein samples (60 μg/lane) were separated by 10 or 12% SDS polyacrylamide gel and electrotransferred to nitrocellulose filter membranes. The membranes were blocked with 5% skim milk for 1 h at room temperature and then incubated with primary antibodies overnight at 4 °C. The membranes were then washed with TBST and incubated with horseradish peroxidase (HRP)-conjugated secondary antibody for 2 h at room temperature. The protein bands were visualized using enhanced chemiluminescence (ECL), and the relative protein quantity was determined using ImageJ software (National Institutes of Health, USA). The primary antibodies used include the following: Albumin (Sigma, USA) and β-tubulin (Sigma, USA) as a loading control. HRP-conjugated anti-IgG (Sigma, USA) was used as secondary antibodies.

As described in the previous study, with the exposure of various concentrations of DDD and Normal Saline, rats were injected with 1% sodium pentobarbital, the intact brain tissues removed immediately. The brain tissues were divided into two hemispheres along the midline. After the blood clot was gently removed with cotton swabs and moisture on the brain surface was dried by filter paper, brain tissues were immediately weighted with an electronic analytical balance and the wet weight was recorded (the weight was accurate to 0.1 mg). The brain tissues were then dried in an electric thermostatic drier at 100 ± 5 °C for 72 h until the sample weights were consisted to obtain the dry weight and calculated as follows: water content of brain tissues = (wet weight - dry weight)/(wet weight) × 100%.

Protein Samples Preparation

Prepared brain tissue (cerebral cortex of the affected side) was dissected into small pieces and mixed with appropriate PMSF + RIPA, homogenized at low temperature, fractionated on ice, then centrifuged at high speed. The supernatant was then extracted and separated into 1.5 mL EP and stored at −20 °C.

For digestion, the protein solution was reduced using 5 mM dithiothreitol for 30 min at 56 °C and alkylated using 11 mM iodoacetamide for 15 min at room temperature in the dark. The protein sample was then diluted by adding 100 mM TEAB to a urea concentration of < 2 M. Finally, trypsin was added at a 1:50 trypsin-to-protein mass ratio for the first digestion overnight and 1:100 trypsin-to-protein mass ratio for the second 4 h digestion.

TMT Labeling and HPLC Fractionation

The digested peptides were desalted using a Strata X C18 SPE column (Phenomenex, USA) and vacuum-dried. Peptides were dissolved in 0.5 M TEAB and labeled using the tandem mass tag (TMT) kit (Thermo Fisher Scientific, USA) according to the manufacturer's instructions. The labeled peptides were fractionated by high pH reverse-phase HPLC using an Agilent 300 Extend C18 column (5μm, 4.6×250 mm). Peptides were first separated using a gradient of 8% to 32% acetonitrile (pH 9.0; Fisher Chemical, USA) over 60 min into 60 fractions, which were then combined into nine fractions and dried by vacuum centrifugation.

LC-MS/MS Analysis

Peptides were dissolved in liquid chromatography with mobile phase A (0.1% (v/v) formic acid aqueous

solution) and separated using the EASY-NLC 1000 UPLC system. Mobile phase A: A solution containing 0.1% formic acid and 2% acetonitrile. Mobile phase B: A solution containing 0.1% formic acid and 90% acetonitrile. Liquid phase gradient settings were: 0–50 min, 7–16% B; 50–85 min, 16–30% B; 85–87 min, 30–80% B; 87–90 min, 80% B, the flow rate was maintained at 400 nL/min. The peptides were analyzed using Orbitrap Fusion Lumos mass spectrometry. The scanning range and resolution of primary mass spectrometry was 350–1550 m/z, 60,000. The scanning range and resolution of secondary mass spectrometry was 100 m/z, 30,000. In the data acquisition mode, the top ten peptide parent ions with the highest signal intensity were selected to enter the HCD collision cell successively for fragmentation with 32% fragmentation energy, and second-level mass spectrometry analysis was sequentially performed.

Database Research

Secondary mass spectral data were retrieved using MaxQuant (v1.5.2.8). The retrieval parameters were as follows: UniProt RAT was used to calculate the false positive rate caused by random matching. A common contaminant database was added to eliminate the influence of contaminant proteins in the identification results. The minimum length of the peptide segment was set to seven amino acid residues. The mass error tolerance of the primary parent ions for the first and main searches was set to 20, and 5 PPM, respectively, while the mass error tolerance of the secondary fragment ions was 0.02. The quantitative method was set as TMT-10PLEX, and the FDR of protein identification and PSM identification was set at 1%.

Repeatability Test

Principal component analysis, relative standard deviation, and Pearson correlation coefficient were used to evaluate whether the quantitative reproducibility of the protein was statistically significant.

Definition and Annotation of Differential Protein Expression and Enrichment Analysis

Differential protein expression was identified by determining the number of upregulated and downregulated proteins in each comparison group by setting 1.2 and 1/1.2 times as fold change thresholds, with a statistical p-value < 0.05.

Annotation of differential proteins from Gene Ontology (GO) were then classified as being related to Biological Processes (BP), Molecular Functions (MF), or Cellular Components (CC), and subcellular localization was determined to annotate the biological role and protein localization.

Functional enrichment analysis was performed based on GO, and Kyoto Encyclopedia of Genes and Genomes (KEGG) pathways, with a $p < 0.05$ (two-tailed Fisher's exact test) considered to be statistically significant. One-way hierarchical clustering was conducted for the differentially expressed proteins based on the significant enrichments using the "heatmap.2" function from the "gplots" R-package.

Differentially Expressed Proteins Quantification by Parallel Reaction Monitoring (PRM)

Differentially expressed proteins were selected for validation using the RPM. RPM mass spectrometric analysis was performed using tandem mass spectrometry (MS/MS) in Q Exactive™ Plus (Thermo, USA) coupled online to the UPLC. Protein exaction, tryptic digestion, LC parameters, electrospray voltage, scan range, and Orbitrap resolution were performed in the same way as in the TMT experiment. The AGC for full MS was set at 20 M, and MS/MS was set at auto. The isolation window for MS/MS was set at 2.0 m/z. The resulting MS data were processed using Skyline (V.3.6). After normalizing the quantitative information, a relative quantitative analysis was performed on the target peptides.

Statistical Analysis

All data are presented as mean ± standard deviation (SD). Data were analyzed using Student's t-test and one-way analysis of variance (ANOVA), followed by Scheffe's post-hoc test. One-way multivariate ANOVA was performed to determine significant differences in biochemical parameters between the control and sample groups. Differences were considered statistically significant at $p < 0.05$.

Results

Effect of DDD on the Neurological Outcomes in AICH Rats

On the first day, four groups subjected to injection of autologous blood into the caudate nucleus to induce AICH, showed similar neurological deficits, while animals in the

control group were relatively free of neurological impairments. Evaluation of mNSS at different time points revealed that the neurological statuses in both the model and DDD-treated groups improved with time (mNSS decreased). The mNSS scores in the high-dose group were significantly lower than those in the medium-dose, low-dose, and model groups on days 1, 3, and 7, with statistically significant difference ($p < 0.05$), especially on day 7 (shown in Figure 1).

HE Staining results

Non-necrotic cells in the cortex and medulla of normal rats were observed under a light microscope in the animal control group. Additionally, these animals did not exhibit blood injection into the brain, nor inflammatory infiltration from the semi-dark area, and had normal microscopic features. Conversely, pathological features revealed obvious bleeding around the stove, inflammatory cell infiltration, and edema around visible necrotic nerve cells, in the model group. Compared with the AICH model group, the low-, medium-, and high-dose groups at 3 and 7 days exhibited more remarkable pathological features, including hematoma formation, edema absorption, and an anti-ischemic response of peripheral nerve cells in the ischemic area. Furthermore, the necrotic nerve cells around the lesion were significantly reduced. These results were particularly evident on day 7 in the high-dose group (shown in Figure 2).

BBB Injury and Brain Water Content

We evaluated the levels of albumin in each group, which is an important hallmark of BBB disruption. In the model group, albumin levels in the brain tissues were significantly increased when compared with the control group, while the low-, medium-, and high-dose DDD treatment at 7 days significantly reduced the albumin induced by ICH, furthermore DDD high-dose at 7 days did not increase the albumin (shown in Figure 3A–B). For brain water content, the model group showed significant increases compared with the control group, while DDD treatment significantly impaired the brain water content. Compared with ICH model group, the low-, medium-, and high-dose groups at 3 and 7 days were significantly impaired the brain water content, especially DDD high-dose treatment at 7 days compared with control group (shown in Figure 3C). These results indicated that 7 days high-dose DDD treatment is able to ameliorate brain injury (including neurological outcomes, BBB disruption, and brain edema) after ICH and it did not damage BBB. This rehabilitation of the BBB integrity might be an important contributing factor to the reduction of brain edema following DDD treatment.

Functional Characterization of Differentially Expressed Proteins and Enrichment Analysis

Considering that the strongest effect was observed after 7 days of exposure to high-dose DDD, all subsequent experiments were conducted under these conditions unless otherwise indicated. The differentially expressed proteins (high-dose versus model group) were classified according to their subcellular localization (shown in Figure 4A). Approximately 26.97% of the differentially expressed proteins were present in the extracellular matrix, including collagen alpha-1 (I).

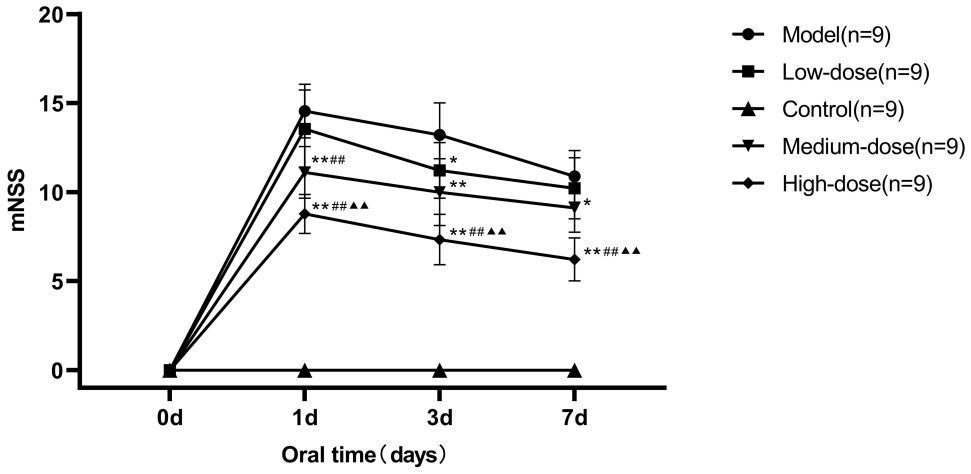

Figure 1 Effect of DDD on neurological outcomes in AICH rats. *Compared with the model group, $p < 0.05$; **Compared with the model group, $p < 0.01$; ##Compared with the low-dose group, $p < 0.01$; ▲▲Compared with the medium-dose group, $p < 0.01$. Data were analyzed using Student's *t*-test and one-way analysis of variance (ANOVA), followed by Scheffe's post-hoc test.

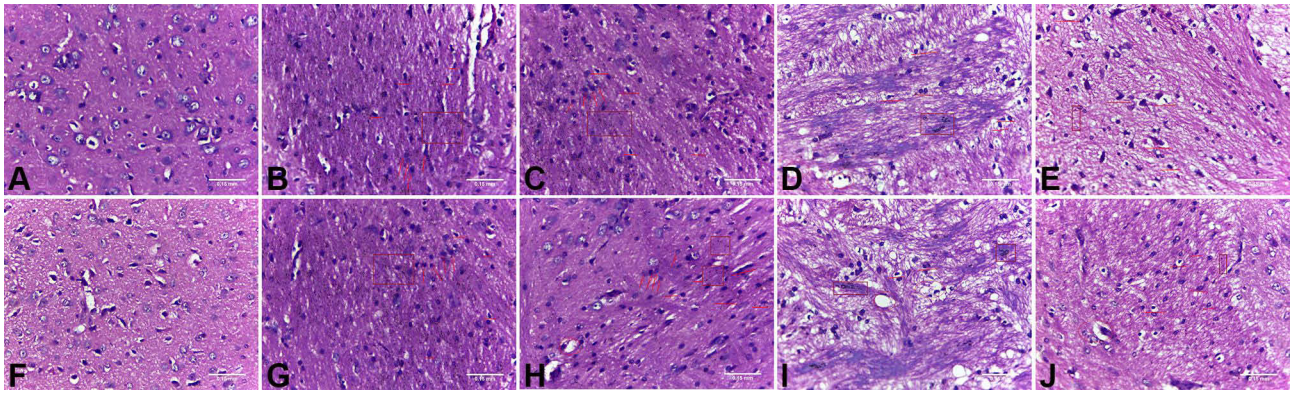

Figure 2 HE staining. (**A**) Control group at day 3; (**B**) Model group at day 3; (**C**) Low-dose group at day 3; (**D**) Medium-dose group at day 3; (**E**) High-dose group at day 3; (**F**) Control group at day 7; (**G**) Model group at day 7; (**H**) Low-dose group at day 7; (**I**) Medium-dose group at day 7; (**J**) High-dose group at day 7. (Box: evident bleeding foci and bleeding points. Arrow: Inflammatory cell infiltration. Straight-line: typical nerve cell morphology. Circle: vacuolar degeneration appears.).

GO classification (BP, MF, CC) and KEGG enrichment were then performed in each group, and cluster analysis was performed to determine the correlation between protein functions and differential expression. Results were visualized as heat maps. BP enrichment analysis demonstrated that upregulated proteins were primarily associated with the sensory perception of mechanical stimulus. In contrast, downregulated proteins were found to be largely associated with response to bacteria, inflammatory response to antigenic stimuli, and leukocyte aggregation (shown in Figure 4B). Concerning MF, downregulated proteins were associated with Toll-like receptor 4 binding and antioxidant activity (shown in Figure 4C). Meanwhile, for the CC, centrosome, and nuclear chromosome were primarily clustered in downregulated proteins (shown in Figure 4D).

To further explore the pathway of DDD during AICH at 7 days, KEGG pathway enrichment analysis was carried out, and the upregulated proteins were found to be primarily enriched in the PI3k-Akt and AGE-RAGE signaling pathway (shown in Figure 4E). Meanwhile, the downregulated proteins were mainly enriched in the IL-17 signaling pathway (shown in Figure 4F).

These results suggest that the mechanism of DDD during AICH at 7 days in the high-dose group might be related to positive regulation of adaptive immune responses, leukocyte aggregation, and regulation of inflammation-related signaling pathways.

Differentially Expressed Protein Selection

Venn diagrams were used to identify significantly upregulated and downregulated proteins before and 7 days after DDD administration (shown in Figure 5). Among them, 23 proteins were upregulated in the model versus the control group while downregulated in the high-dose versus model group analysis. Thirteen proteins were downregulated in the model versus control group while upregulated in the high-dose versus model group. Hierarchical clustering was conducted among the three repeated samples for the above 36 proteins, and a heat map was constructed. Results suggested that these proteins may have similar functions and participate in certain related metabolic processes or signaling pathways (shown in Figure 6).

Among these 36 proteins, S100a8 and S100a9 were decreased by 0.614 and 0.506 times while Col1a1 and Col1a2 were increased by 1.319 and 1.348 times after 7-day exposure to DDD. Specific protein information is shown in Table 1.

The S100 family is a group of low-molecular-weight modified binding proteins with similar structures and functions. S100a8 and S100a9 are two critical members of the S100 family, which primarily exert their biological function when forming a heterodimer S100a8/a9.[17] S100a8 and S100a9 play roles in a wide range of biological processes, such as apoptosis, immune-inflammatory response, and embryonic development.[18] Under abnormal conditions such as microbial infection, inflammation, activated immune cells secrete S100a8 and S100a9 to further activate the immune system and transmit signals to macrophages[19] which can also stimulate inflammatory cells to release inflammatory factors, thus, directly participating in the acute and chronic inflammatory response.[20,21] Collagen type I is an important member of the family and a key structural component of the extracellular matrix,[22] as subcellular location results. It usually consists of collagen type I α1 chains (Col1a1) and collagen type I α2 chains (Col1a2). The expression and deposition

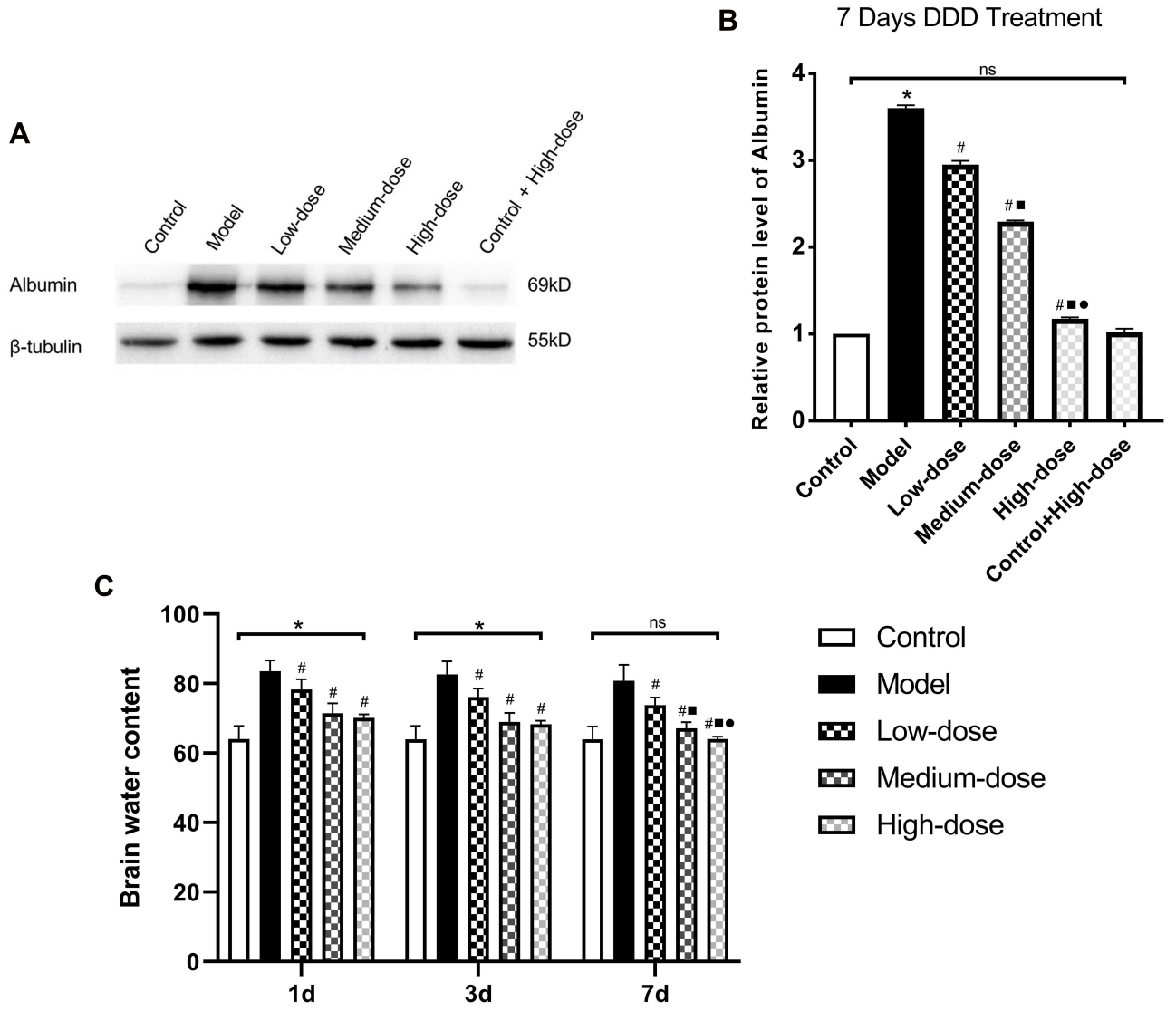

Figure 3 Evaluation of BBB disruption and brain water content of brain. (**A**) Western blot analysis examines the albumin level of the Control, Model, DDD Low-dose group at day 7, DDD Medium-dose group at day 7, DDD High-dose group at day 7, Control group after 7 days of exposure to DDD; (**B**) Relative albumin levels were calculated based on densitometry analysis. The mean albumin level of the control group was normalized to 1.0; (**C**) Recorded brain water content after 1,3,7 days of exposure to DDD (Low-dose, Medium-dose, High-dose); *Compared with Control group, $p < 0.05$; # Compared with Model group, $p < 0.05$; ■Compared with Low-dose group, $p < 0.05$; ●Compared with Medium-dose group, $p < 0.05$, ns deemed as no significant difference, n = 9.

of collagen can affect cell functions such as proliferation, adhesion, migration, and invasion.[23,24] Col1a1 and Col1a2 affect blood vessel development, particularly artery development, venous blood vessel development and blood vessel maturation. While abnormal development and even vascular malformation can lead to intracerebral hemorrhage events. The functions of these four proteins correlated with the results obtained by bioinformatics analysis; therefore, the mechanism of neuroprotective action of DDD during AICH in SD rats may be mediated by regulating these proteins. Nevertheless, these results should be further validated.

Validation of Target Proteins by PRM

PRM was quantified based on the peak area. In this experimental design, more than two unique peptides were used for each protein quantification. Only one peptide segment was identified for some proteins due to sensitivity and other reasons. PRM quantification was performed for the target proteins. The results of the PRM showed that the four differentially expressed proteins, namely S100a8 (shown in Figure 7A), S100a9 (shown in Figure 7B and C), Col1a1 (shown in Figure 7D), and Col1a2 (shown in Figure 7E and F), exhibited trends similar to those observed using quantitative proteomics, and all results were statistically significant.

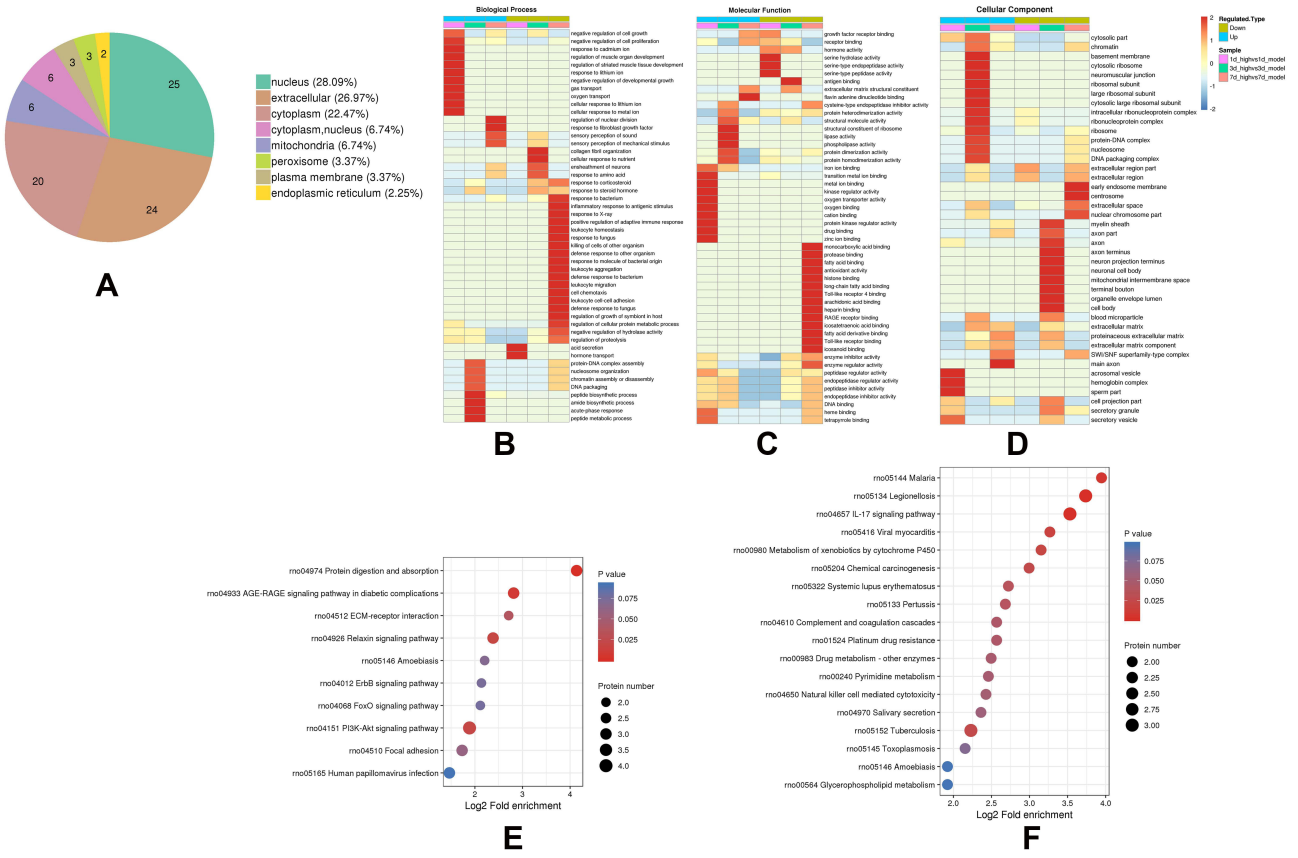

Figure 4 Functional characterization of differentially expressed proteins and enrichment analysis. (**A**) Subcellular localization; (**B–D**) Cluster analysis heat map of the differentially expressed proteins according to GO (BP. MF. CC); (**E** and **F**) Cluster analysis heat map of proteins with upregulated and downregulated expression after 7 days of exposure to DDD based on KEGG enrichment. Red indicates a strong degree of enrichment (the deeper the red is, the stronger the enrichment is). The blue color indicates a weaker degree of enrichment (the lighter the blue is, the weaker the enrichment is).

Discussion

DDD is a representative prescription that has been used for more than 1800 years for promoting blood circulation and removing blood stasis, purging and clearing the viscera; it was first recorded in "Treatise on febrile diseases." Indeed, DDD, which consists of rhubarb, peach kernel, leech, and gadfly, has proven effective against seemingly incurable diseases, including intracerebral hemorrhage. Specifically, leech serves to remove blood stasis without negatively impacting newly produced blood as it only affects the blood phase without interfering with Qi. Meanwhile, gadfly governs blood extravasation and promotes blood circulation, throughout the nine orifices. Considering that leech is a monarch drug, and gadfly is a ministerial drug, combined use of both can effectively address blood accumulation. Additionally, peach kernel is considered an assistant drug and can reduce blood stagnation while helping to produce new blood. Similarly, rhubarb can eliminate blood stasis while also purging the intestines and stomach. Hence, the combined use of peach kernel and rhubarb can eliminate blood stasis through the lower orifices. Combining all four compounds can realize the efficacy of promoting blood circulation to remove blood stasis and purge fu-organs(viscera). However, the precise associated molecular mechanisms remain unclear.

In this study, we investigated the neuroprotective mechanism of DDD in rats with AICH. Hemorrhagic stroke is a particularly devastating condition with greater morbidity and mortality than ischemic stroke.[25] Globally, 13.7 million strokes occurred in 2016, of which 30% were hemorrhagic stroke.[26] According to Canadian stroke best practice recommendations: Management of Spontaneous Intracerebral Hemorrhage, 7th Edition Update 2020,[27] following a confirmed diagnosis, one of the most important early therapeutic strategies is to limit hematoma expansion, which is a strong determinant of early neurological deterioration and poor clinical outcomes.[28] In the current study, compared with the AICH model group, the low-,

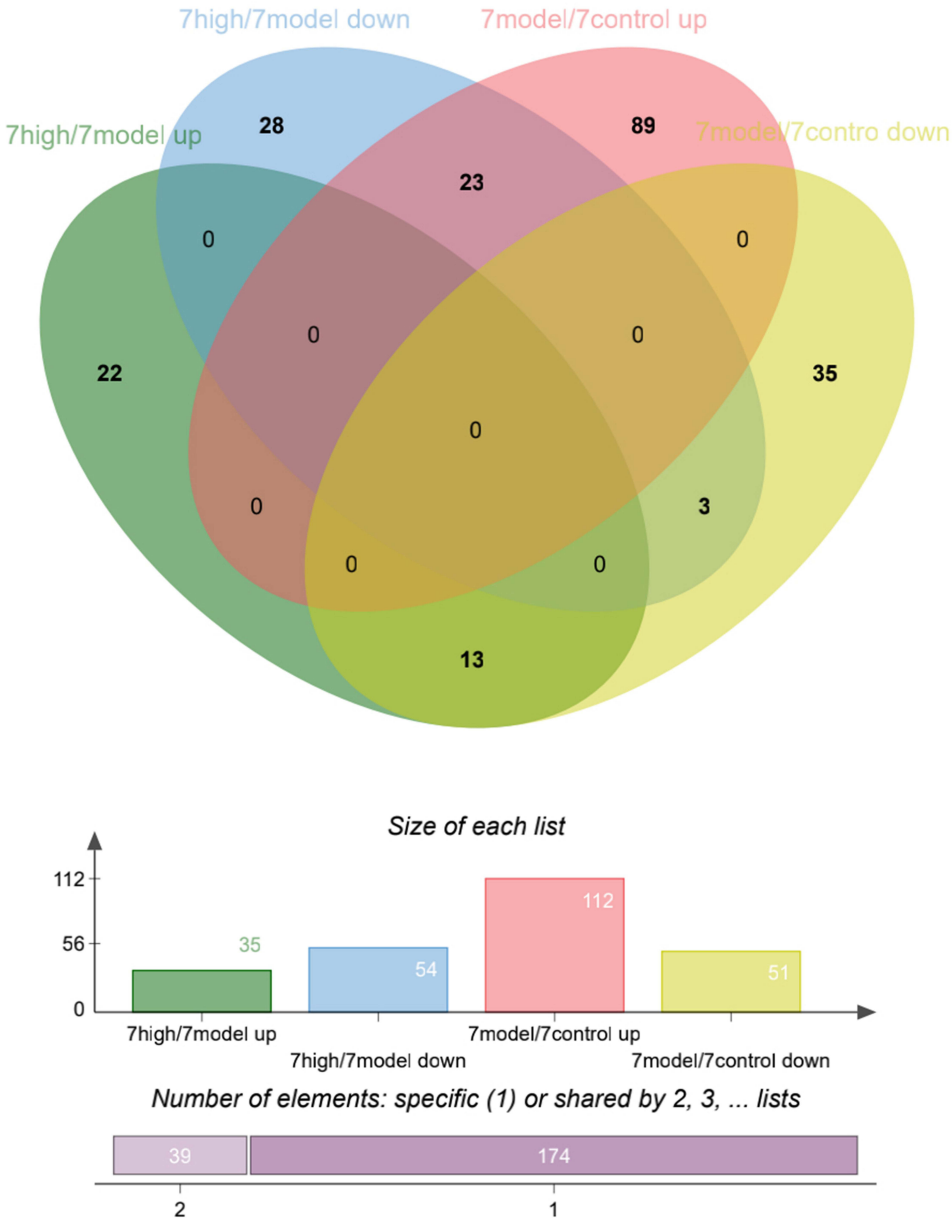

Figure 5 Differentially expressed protein distribution before and after 7 days of exposure to DDD.

medium-, and high-dose groups at 3 and 7 days showed significant improvements in limiting hematoma expansion, edema absorption, and the anti-ischemic response of peripheral nerve cells in the ischemic area. Moreover, the necrotic nerve cells around the lesion were significantly reduced. These results were particularly strong in the high-dose group after 7 days of exposure to DDD. Using the mNSS score, we found that high-dose DDD exposure of 7 days had a powerful effect on improving neurological deficits and rehabilitating the BBB integrity. These results demonstrate that the application of DDD positively impacts AICH.

Through bioinformatics analysis, these results suggest that the mechanism of DDD during AICH at 7 days might be related to positive regulation of the adaptive immune response, leukocyte aggregation, and regulated signaling pathway associated with inflammatory. Next, Venn diagrams were used to identify which proteins were significantly upregulated and downregulated before and 7 days after DDD exposure. Among them, 23 proteins were upregulated in the model versus control group and downregulated in the high-dose versus model group. Thirteen proteins were downregulated in the model versus control group and upregulated in the high-dose versus model group. In particular,

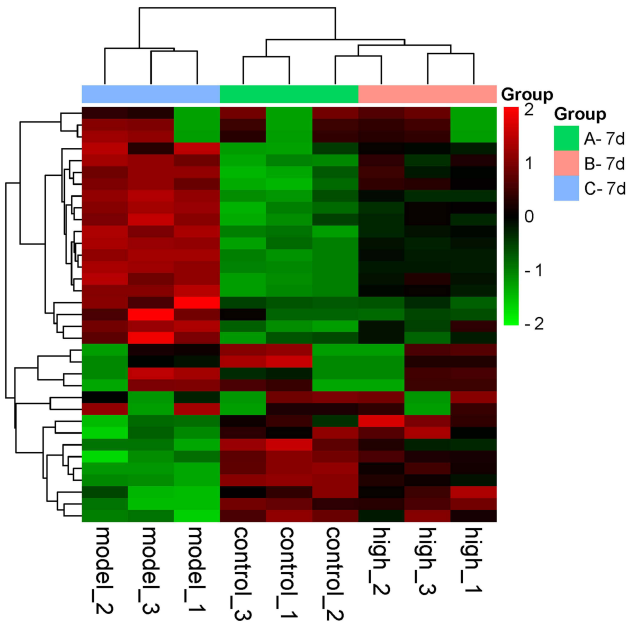

Figure 6 Cluster analysis heat map of 36 differentially expressed proteins. Red represents proteins with upregulated expression, and the green represents proteins with downregulated expression. The tree diagram at the top represents cluster analysis results of different samples in different experimental groups. The tree diagram on the left represents the cluster analysis results of different genes from different samples.

relative to the control group, S100a8 S100a9 were upregulated 3.316 and 4.957 times in the model group but downregulated 0.614 and 0.506 times in the high-dose group relative to the model group. Col1a1 Col1a2 were downregulated 0.677 and 0.598 times in the model group relative to the control group but upregulated 1.319 and 1.348 times in the high-dose group compared to the model group.

The S100a8/a9 protein is a heterodimer composed of the light chain S100a8 (molecular weight: 10,000) and a heavy chain S100a9 (molecular weight: 14,000) proteins. S100a8 and S100a9 are mainly expressed in myeloid cells.[17] According to structural studies, the S100A8/A9 protein complex contains two EF-hand structures connected by a hinge region.[29] Infection-induced inflammation following infection with bacteria causes neutrophils, macrophages, and monocytes to express and secrete S100a8/a9.[30] S100a8/a9 can promote inflammatory cell infiltration via release of inflammatory cytokines, causing neutrophil aggregation at the site of inflammatory injury, then macrophages can then be released. S100a8/a9 produces a positive feedback effect, thereby amplifying the inflammatory response.[31] The early expression of S100 proteins during infection-induced inflammation suggests that S100a8 and S100a9 trigger TLR-4 or RAGE-mediated multiple inflammatory pathways.[32] These considerations were consistent with the results of BP, MF, and KEGG enrichment analysis. Subsequently, the nuclear κB transcription signaling pathway is activated to stimulate downstream pro-inflammatory cytokines and inflammatory mediators.[33] Our findings showing that protein levels of S100a8 and S100a9 in the DDD high-dose group at 7 days were lower than those in the model group were consistent with the results of PRM omics identification, indicating that DDD may inhibit inflammatory cell infiltration, release of inflammatory cytokines, and reduce the inflammatory response.

Collagen type I is the most abundant fibrillar collagen in vertebrates and has long been involved in aneurysm pathogenesis. Collagen type I is encoded by Col1a1 and Col1a2, which express α1(I) and α2(I). Polymorphisms in these genes have been confirmed to be associated with vascular diseases.[34] The association analysis of primary cerebral hemorrhage conducted by Ming et al confirmed that the rs42524 locus polymorphism of the Col1a2 gene significantly correlated with the occurrence of primary intracerebral hemorrhage.[35,36] Yoneyama et al speculated that the Col1a2 gene polymorphism might account for the formation of aneurysms by affecting the fragility and elasticity of the vascular wall and the interaction between other molecules, ultimately changing the strength of the vascular wall, finally causing ICH.[37] Col1a2 is a significant risk factor for intracranial aneurysm susceptibility, with a particularly strong effect in the Asian population.[38] Lindahl et al showed that genetic variants of Col1a2 were the risk factors for stroke and myocardial infarction.[39] Collagen type I-associated abnormalities are found in a wide range of diseases, and several candidate genes have been identified in relation to thoracic aortic aneurysms and bicuspid aortic

Table 1 The Expression of Target Proteins Before and After 7-Day Exposure to DDD

Protein Accession Number	Gene	Description	Fold Change 1	*p*-value 1	Fold Change 2	*p*-value 2
P50115	S100a8	Protein S100-A8	0.614	0.033702	3.316	0.014244
A0A0H2UHJ1	S100a9	Protein S100-A9	0.506	0.000024	4.957	0.000063
P02454	Col1a1	Collagen α-1 chain	1.319	0.000184	0.677	0.000025
F1LS40	Col1a2	Collagen α-2 chain	1.348	0.014097	0.598	0.005657

Note: Fold change 1 and P-valve 1 represent high-dose group versus model group. Fold change 2 and P-valve 2 represent model group versus control group.

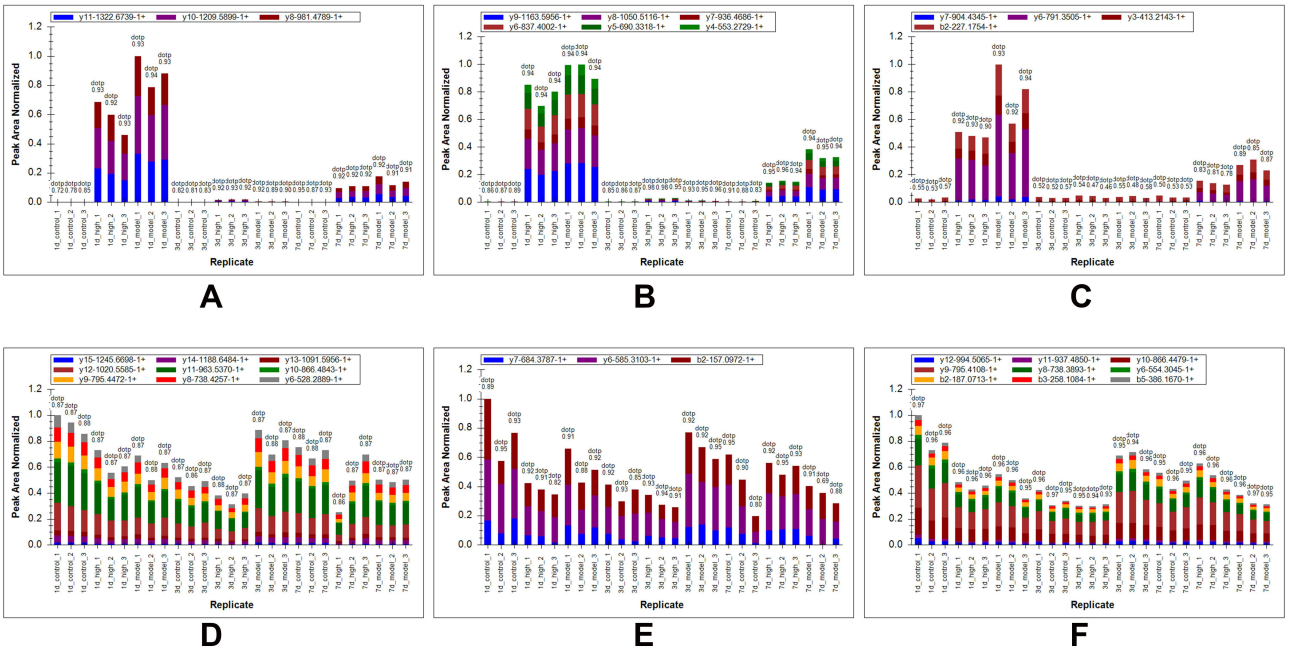

Figure 7 Validation of target proteins by PRM. (**A**) Area distribution of ion peak corresponding to the peptide of S100a8; (**B** and **C**) Different peptides' area distribution of ion peak corresponding to S100a9; (**D**) Area distribution of ion peak corresponding to the peptide of Col1a1; (**E** and **F**) Different peptides' area distribution of ion peak corresponding to Col1a2.

valves.[40,41] Due to the wide distribution of collagen type I in the body, the effects of genetic variants may also affect vascular walls and other tissues. It should also be noted that these patients sometimes develop aortic dissection,[35] which is often associated with hypertension and arteriosclerosis. These two factors are always considered as risk factors for AICH. The protein expression of Col1a1 and Col1a2 in the DDD high-dose group at 7 days was higher than that in the model group, which was also consistent with the results of PRM omics identification, indicating that the DDD mechanism of action may be related to genetic polymorphisms and blood vessel development.

Base on current research, we propose the conjecture that DDD may exert protective effect against AICH stroke in rats by downregulating S100a8 and S100a9 to inhibit inflammatory cell infiltration and release inflammatory cytokines. Besides, DDD also may act by upregulating Col1a1 and Col1a2 to affect blood vessel development. Additionally, we plan to conduct follow-up experiments on modification proteomics to study the mechanism of DDD.

Conclusions

Applying a high-dose of DDD for 7 days in rats with AICH stroke exerted neurological protection by upregulating Col1a1 Col1a2 and downregulating S100a8 S100a9 proteins.

Data Sharing Statement

All data generated or analyzed during this study are included in this article.

Statement of Ethics

This study protocol was reviewed and approved by the Animal Ethics Committee of Changchun University of Traditional Chinese Medicine (Approval No.: 20180008). All animal experimental procedures were performed in accordance with the guidelines of the National Institutes of Health on the care and use of animals. Animals were housed in an Association for Assessment and Accreditation of Laboratory Animal Care International (AAALAC)-approved animal quarters in our hospital with a controlled temperature of 25 °C and 12 h light-dark cycles.

Acknowledgments

The authors thank Tianyi Zhuang for assistance with language editing and Jingjie PTM BioLab (Hangzhou) Co. Ltd for assistance with mass spectrometry.

Author Contributions

All authors made a significant contribution to the work reported, whether that is in the conception, study design, execution, acquisition of data, analysis, and interpretation,

or in all these areas; took part in drafting, revising, or critically reviewing the article; gave final approval of the version to be published; have agreed on the journal to which the article has been submitted; and agree to be accountable for all aspects of the work.

Funding

This study was supported by the Science and Technology Development Program of Jilin Province [No. 20180101160JC].

Disclosure

The authors have no conflicts of interest to declare.

References

1. Li Y, Fang W, Tao L, et al. Efficacy and safety of intravenous nimodipine administration for treatment of hypertension in patients with intracerebral hemorrhage. *Neuropsychiatr Dis Treat*. 2015;11:1231–1238. doi:10.2147/NDT.S76882
2. van Asch CJ, Luitse MJ, Rinkel GJ, van der Tweel I, Algra A, Klijn CJ. Incidence, case fatality, and functional outcome of intracerebral haemorrhage over time, according to age, sex, and ethnic origin: a systematic review and meta-analysis. *Lancet Neurol*. 2010;9(2):167–176. doi:10.1016/S1474-4422(09)70340-0
3. Wang W, Jiang B, Sun H, et al. Prevalence, Incidence, and Mortality of Stroke in China: results from a Nationwide Population-Based Survey of 480 687 Adults. *Circulation*. 2017;135(8):759–771. doi:10.1161/CIRCULATIONAHA.116.025250
4. Sze KH, Wong E, Or KH, Lum CM, Woo J. Factors predicting stroke disability at discharge: a study of 793 Chinese. *Arch Phys Med Rehabil*. 2000;81(7):876–880. doi:10.1053/apmr.2000.6279
5. Garg R, Biller J. Recent advances in spontaneous intracerebral hemorrhage. *F1000Research*. 2019;2:8.
6. Cui HJ, Yang AL, Zhou HJ, et al. Buyang huanwu decoction promotes angiogenesis via vascular endothelial growth factor receptor-2 activation through the PI3K/Akt pathway in a mouse model of intracerebral hemorrhage. *BMC Complement Altern Med*. 2015;15:91. doi:10.1186/s12906-015-0605-8
7. Ren J, Zhou X, Wang J, Zhao J, Zhang P. Poxue Huayu and Tianjing Busui Decoction for cerebral hemorrhage (Upregulation of neurotrophic factor expression): upregulation of neurotrophic factor expression. *Neural Regen Res*. 2013;8(22):2039–2049.
8. Huang Q, Lan T, Lu J, et al. DiDang Tang Inhibits Endoplasmic Reticulum Stress-Mediated Apoptosis Induced by Oxygen Glucose Deprivation and Intracerebral Hemorrhage Through Blockade of the GRP78-IRE1/PERK Pathways. *Front Pharmacol*. 2018;9:1423. doi:10.3389/fphar.2018.01423
9. Lu J, Huang Q, Zhang D, et al. The Protective Effect of DiDang Tang Against AlCl3-Induced Oxidative Stress and Apoptosis in PC12 Cells Through the Activation of SIRT1-Mediated Akt/Nrf2/HO-1 Pathway. *Front Pharmacol*. 2020;11:466. doi:10.3389/fphar.2020.00466
10. Li YB, Cui XN, Li Y, Pan L, Wen JY. Effect of two Chinese medicinal compounds, blood-activating and water-draining medicine, on tumor necrosis factor alpha and nuclear factor kappa B expressions in rats with intracerebral hemorrhage. *Chin J Integr Med*. 2014;20(11):857–864. doi:10.1007/s11655-012-1081-3
11. Wang Y, Peng F, Xie G, et al. Rhubarb attenuates blood-brain barrier disruption via increased zonula occludens-1 expression in a rat model of intracerebral hemorrhage. *Exp Ther Med*. 2016;12(1):250–256. doi:10.3892/etm.2016.3330
12. Qi HY, Li L, Yu J, et al. Proteomic Identification of Nrf2-Mediated Phase II Enzymes Critical for Protection of Tao Hong Si Wu Decoction against Oxygen Glucose Deprivation Injury in PC12 Cells. *Evid Based Complement Alternat Med*. 2014;2014:945814. doi:10.1155/2014/945814
13. Adjei AA. Novel small-molecule inhibitors of the vascular endothelial growth factor receptor. *Clin Lung Cancer*. 2007;8(Suppl 2):S74–8. doi:10.3816/CLC.2007.s.005
14. Fleegal-DeMotta MA, Doghu S, Banks WA. Angiotensin II modulates BBB permeability via activation of the AT(1) receptor in brain endothelial cells. *J Cereb Blood Flow Metab*. 2009;29(3):640–647. doi:10.1038/jcbfm.2008.158
15. Dang B, Li H, Xu X, et al. Cyclophilin A/Cluster of Differentiation 147 Interactions Participate in Early Brain Injury After Subarachnoid Hemorrhage in Rats. *Crit Care Med*. 2015;43(9):e369–81. doi:10.1097/CCM.0000000000001146
16. Kumar A, Mittal R, Khanna HD, Basu S. Free radical injury and blood-brain barrier permeability in hypoxic-ischemic encephalopathy. *Pediatrics*. 2008;122(3):e722–7. doi:10.1542/peds.2008-0269
17. Wang S, Song R, Wang Z, Jing Z, Wang S, Ma J. S100A8/A9 in Inflammation. *Front Immunol*. 2018;9:1298. doi:10.3389/fimmu.2018.01298
18. Pruenster M, Vogl T, Roth J, Sperandio M. S100A8/A9: from basic science to clinical application. *Pharmacol Ther*. 2016;167:120–131. doi:10.1016/j.pharmthera.2016.07.015
19. Vogl T, Ludwig S, Goebeler M, et al. MRP8 and MRP14 control microtubule reorganization during transendothelial migration of phagocytes. *Blood*. 2004;104(13):4260–4268. doi:10.1182/blood-2004-02-0446
20. Katano M, Okamoto K, Suematsu N, et al. Increased expression of S100 calcium binding protein A8 in GM-CSF-stimulated neutrophils leads to the increased expressions of IL-8 and IL-16. *Clin Exp Rheumatol*. 2011;29(5):768–775.
21. Muroi M, Tanamoto K. TRAF6 distinctively mediates MyD88- and IRAK-1-induced activation of NF-kappaB. *J Leukoc Biol*. 2008;83(3):702–707. doi:10.1189/jlb.0907629
22. Li ZL, Wang ZJ, Wei GH, Yang Y, Wang XW. Changes in extracellular matrix in different stages of colorectal cancer and their effects on proliferation of cancer cells. *World J Gastrointest Oncol*. 2020;12(3):267–275. doi:10.4251/wjgo.v12.i3.267
23. Wu Y, Xu Y. Integrated bioinformatics analysis of expression and gene regulation network of COL12A1 in colorectal cancer. *Cancer Med*. 2020;9(13):4743–4755. doi:10.1002/cam4.2899
24. Jones VA, Patel PM, Gibson FT, Cordova A, Amber KT. The Role of Collagen XVII in Cancer: squamous Cell Carcinoma and Beyond. *Front Oncol*. 2020;10:352. doi:10.3389/fonc.2020.00352
25. Krishnamurthi RV, Moran AE, Forouzanfar MH, et al. The global burden of hemorrhagic stroke: a summary of findings from the GBD 2010 study. *Glob Heart*. 2014;9(1):101–106. doi:10.1016/j.gheart.2014.01.003
26. Feigin VL, Norrving B, Mensah GA. Global Burden of Stroke. *Circ Res*. 2017;120(3):439–448. doi:10.1161/CIRCRESAHA.116.308413
27. Shoamanesh Co-Chair A, Patrice Lindsay M, Castellucci LA, et al. Canadian stroke best practice recommendations: management of Spontaneous Intracerebral Hemorrhage, 7th Edition Update 2020. *Int J Stroke*. 2021;16(3):321–341. doi:10.1177/1747493020968424
28. Dowlatshahi D, Demchuk AM, Flaherty ML, et al. Defining hematoma expansion in intracerebral hemorrhage: relationship with patient outcomes. *Neurology*. 2011;76(14):1238–1244. doi:10.1212/WNL.0b013e3182143317
29. Wei L, Liu M, Xiong H. Role of Calprotectin as a Biomarker in Periodontal Disease. *Mediators Inflamm*. 2019;2019:3515026. doi:10.1155/2019/3515026
30. Averill MM, Kerkhoff C, Bornfeldt KE. S100A8 and S100A9 in cardiovascular biology and disease. *Arterioscler Thromb Vasc Biol*. 2012;32(2):223–229. doi:10.1161/ATVBAHA.111.236927

31. Shabani F, Farasat A, Mahdavi M, Gheibi N. Calprotectin (S100A8/S100A9): a key protein between inflammation and cancer. *Inflamm Res*. 2018;67(10):801–812. doi:10.1007/s00011-018-1173-4
32. Ometto F, Friso L, Astorri D, et al. Calprotectin in rheumatic diseases. *Exp Biol Med*. 2017;242(8):859–873. doi:10.1177/1535370216681551
33. Sinha P, Okoro C, Foell D, Freeze HH, Ostrand-Rosenberg S, Srikrishna G. Proinflammatory S100 proteins regulate the accumulation of myeloid-derived suppressor cells. *J Immunol*. 2008;181(7):4666–4675. doi:10.4049/jimmunol.181.7.4666
34. Tian DZ, Wei W, Dong YJ. Influence of COL1A2 gene variants on the incidence of hypertensive intracerebral hemorrhage in a Chinese population. *Genet Mol Res*. 2016;15(1). doi:10.4238/gmr.15017369
35. Isotalo PA, Guindi MM, Bedard P, Brais MP, Veinot JP. Aortic dissection: a rare complication of osteogenesis imperfecta. *Can J Cardiol*. 1999;15(10):1139–1142.
36. Meng Q, Hao Q, Zhao C. The association between collagen gene polymorphisms and intracranial aneurysms: a meta-analysis. *Neurosurg Rev*. 2019;42(2):243–253. doi:10.1007/s10143-017-0925-x
37. Yoneyama T, Kasuya H, Onda H, et al. Collagen type I alpha2 (COL1A2) is the susceptible gene for intracranial aneurysms. *Stroke*. 2004;35(2):443–448. doi:10.1161/01.STR.0000110788.45858.DC
38. Gan Q, Liu Q, Hu X, You C. Collagen Type I Alpha 2 (COL1A2) Polymorphism Contributes to Intracranial Aneurysm Susceptibility: a Meta-Analysis. *Med Sci Monitor*. 2017;23:3240–3246. doi:10.12659/MSM.902327
39. Lindahl K, Rubin CJ, Brandstrom H, et al. Heterozygosity for a coding SNP in COL1A2 confers a lower BMD and an increased stroke risk. *Biochem Biophys Res Commun*. 2009;384(4):501–505. doi:10.1016/j.bbrc.2009.05.006
40. Andreassi MG, Della Corte A. Genetics of bicuspid aortic valve aortopathy. *Curr Opin Cardiol*. 2016;31(6):585–592. doi:10.1097/HCO.0000000000000328
41. Lu Y, Zhang S, Wang Y, Ren X, Han J. Molecular mechanisms and clinical manifestations of rare genetic disorders associated with type I collagen. *Intractable Rare Dis Res*. 2019;8(2):98–107. doi:10.5582/irdr.2019.01064